

Seismic Performance of Building Protective Systems: Evaluations from Full-Scale Lab Tests and Actual Earthquake Observations

Kazuhiko KASAI ¹

1. Professor and Director,
Structural Engineering Research Center, Tokyo Institute of Technology, JAPAN
Email: kasai@serc.titech.ac.jp

Abstract

Characteristics and performance of supplementally-damped buildings are discussed based on two major studies such as shake-table tests of full-scale building specimens having various types of dampers, and monitoring and system identification of existing supplementally-damped tall buildings shaken during the 2011 Tohoku-Oki Earthquake. The former gives detailed information on behavior of dampers, frames, components, and distribution of forces and deformations on these elements, which are essential for rational control design. On the other hand, the latter provides the most significant evidence of response control effectiveness. The results from these studies are believed to cause significant change regarding recognition of effectiveness in this new technology.

Keywords: Response Control, Dampers, Monitoring, Displacement and Acceleration Response, Performance curve, System Identification, Tohoku-Oki Earthquake

1. INTRODUCTION

Significant change has taken place in the past three years, regarding recognition of effectiveness in the supplemental damping technology (JSSI Manual 2003, 2005, 2007) for seismic protection of buildings and their contents:

Although this new technology, increasingly used in Japan, still had no conclusive evidence of its superior performance due to its short history, comprehensive results from full-scale shake table tests of buildings with various dampers have been disseminated since 2008 (Kasai et al. 2008b, 2009a, b, 2011a, b, 2012a, b, Ooki et al. 2008, 2009). The shake-table, the largest in the world, is called as E-Defense facility, and was used to test full-scale 5-story buildings with different dampers and without dampers, respectively, applying the ground motion recorded during the 1995 Great Hanshin Earthquake in the small scale to real (catastrophic) level. The building specimen with 12 dampers were instrumented with more than 1,350 sensors, and local responses of member forces and deformations to global responses such as story drifts and accelerations were obtained under the small to catastrophic table motions, and their relations with the seismic input have been studied in details.

As another important data base on the other hand, many acceleration records were obtained during the 2011 Tohoku-Oki Earthquake from the existing buildings with dampers (e.g., Kasai 2011c,d, Kasai et al. 2012c, 2013, Hisada 2011, 2012, Koyama & Kashima 2011, Maseki et al. 2011). The monitored existing buildings were up to 54-story. Obviously, such buildings can never be tested by using the table and imposing the catastrophic ground motions, and only the minor shaking tests had been performed previously. The 2011 quake caused much stronger shaking than ever for such buildings. However, in contrast to the shake-table tests using numerous sensors, such buildings typically have limited number of accelerometers only, from which only the global responses can be estimated. Nevertheless, the data is obviously significant, since it most realistically represents true behavior of the buildings whose gigantic sizes prohibit laboratory test. Follow-up studies on the monitored responses are being performed, and have already provided for the first time the realistic information validating effects of the supplemental damping.

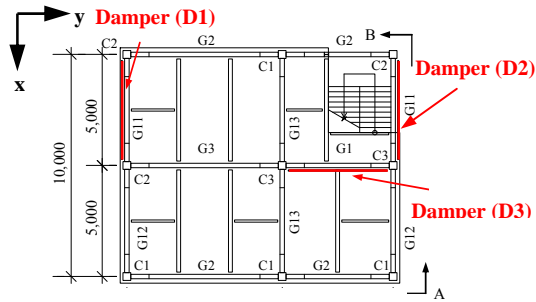
For further growth of the supplemental damping technology, it is important to clarify to what extent the control was effective and how it was achieved using different types of dampers, and above studies and findings are believed to offer the most direct information. The present paper, therefore, addresses the above issues based on results from; (1) shake-table tests of full-scale building specimens having various types of dampers, and (2) monitoring and system identification of existing supplementally-damped buildings shaken due to the Tohoku-Oki Earthquake, respectively.

2. FULL-SCALE SHAKE-TABLE TESTS FOR BUILDINGS WITH DAMPERS

2.1. Building Frame Used

A full-scale 5-story steel frame was constructed and used to validate effectiveness of the supplemental damping technology. The frame as shown in Fig. 1 has two bays in each direction and its overall plan dimension is 10m × 12m. Total height from the upper surface of a stiff foundation beam is 15.8 m (Fig. 1). Seismically active weight of the superstructure is 4,730 kN, including all structural/non-structural components and a portion of live load.

For repeated use of the frame against a series of tests with different types of dampers, the frame was designed not to yield significantly at the controlled story drift angle of 1/100 or less. The frame members of the superstructure consist of rolled or built-up wide-flange beam sections of 400 mm deep, and cold-formed square box column sections of 350 mm × 350 mm. All the beam and column connections were fully-restrained, and the beams were fully composite with 80 mm thick concrete above the 75 mm high corrugated metal deck (Kasai et al. 2009a,b, 2011a, Ooki et al. 2009). Fig. 2 shows exterior views of the building. The precast light-weight curtain walls and glass curtain walls are provided to the 1st and 2nd story levels only. The walls are not attached to the damper bays for ease of dismantling/mantling the dampers. The stairway is detailed to slide during shaking, thereby not producing significant twisting against building. At every story level above the 1st, partitions with doors are constructed. Two types of ceilings with sprinkler systems, as well as mechanical equipment were placed at some story, when the building was tested without dampers at the end test series.



	σ_y (MPa)	σ_u (MPa)
Column (BCR295)	346-398	430-470
	295	400
Beam (SN490B)	331-422	510-557
	325	490
Gusset plate (SN490B)	342-365	510-520
	325	490

Table 2.1 Actual (upper row) and Nominal Steel Yield Stresses

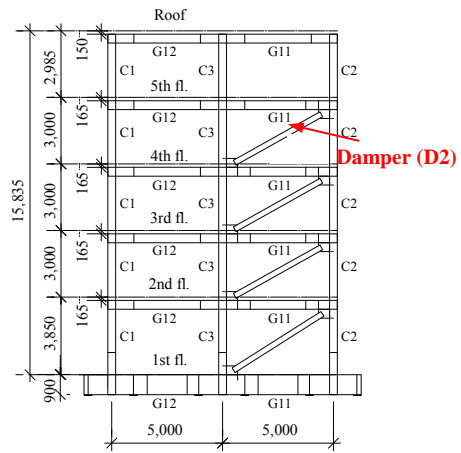
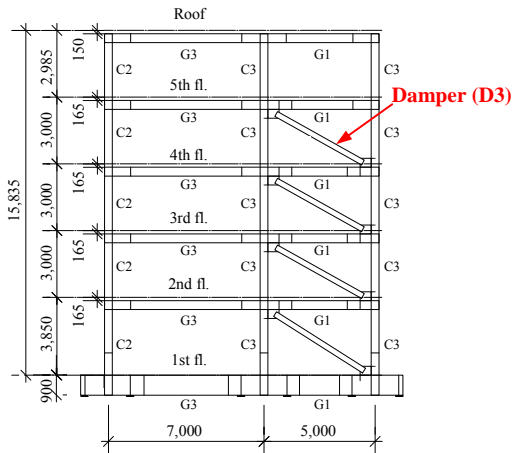


Figure 1 Plan and Elevations of Full-Scale 5-story Building Specimen

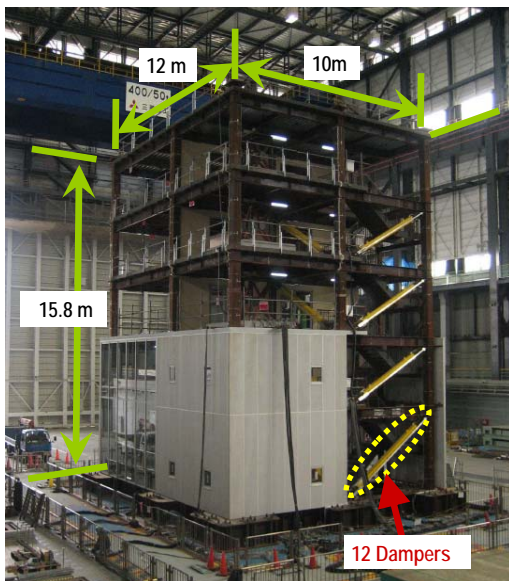


Figure 2 Exterior View of Building Specimen



Figure 3 Four Types of Dampers in Building Specimen (View of Exterior Frame)

2.2. Four Types of Dampers

As shown in Fig. 1, each of 3 bays of the 5-story frame had dampers from 1st to 4th story, thus, 12 dampers of three to four different sizes were used. The test used 4 types of dampers, steel, oil, viscous, and viscoelastic dampers in the order (see Fig. 3). Accordingly, total of 48 (12 dampers x 4 types) dampers were used. The dampers represent major types of dampers in Japan (Fig. 4). Their characteristics are

summarized in Fig. 4, and brief descriptions for the damper types follow (Kasai et al. 2009a, Ooki et al. 2009):

Steel damper utilizes yielding of steel material for energy dissipation. It shows a round curve bounded by bi-linear lines, and can be analytically modeled by using readily available constitutive rules for steel materials. Viscous damper utilizes flow resistance of the polymer liquid. Its force is proportional to the fractional power of velocity, leading to the hysteresis loop of combined ellipse and rectangle. Oil damper utilizes flow resistance of the oil with low viscosity. The damper typically has a relief mechanism to switch viscous coefficient to a small value when subjected to a large velocity, making the hysteresis to switch from an elliptical shape to a rectangle shape. Viscoelastic damper utilizes molecular motion of a polymer for energy dissipation. Hysteresis loop is an inclined ellipse, and the inclination angle and the fatness of the loop depend on the excitation frequency and the temperature.

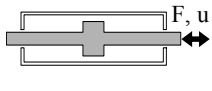
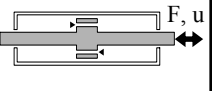
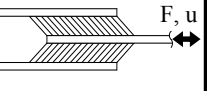
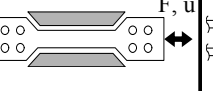
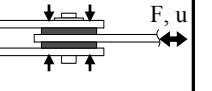
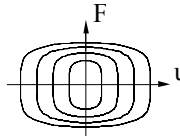
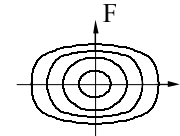
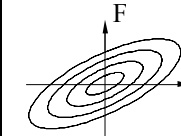
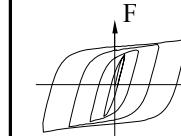
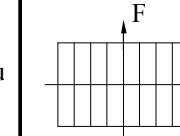
Viscous	Oil	Viscoelastic	Steel	Friction
				
Shear/Flow Resist Panel, Box, Cylinder	Flow Resist Cylinder	Shear Resist Brace, Panel, etc.	Axial/Shear Yielding Brace, Panel, etc.	Slip Resist Brace, Panel
$F = C\dot{u}^\alpha$	$F = C_1\dot{u}$ or $C_2\dot{u}$	$F = K(\omega)u + C(\omega)\dot{u}$	$F = K \cdot f(u)$	$F = K \cdot f(u)$
				

Figure 4 Five Major Types of Dampers Used in Japan

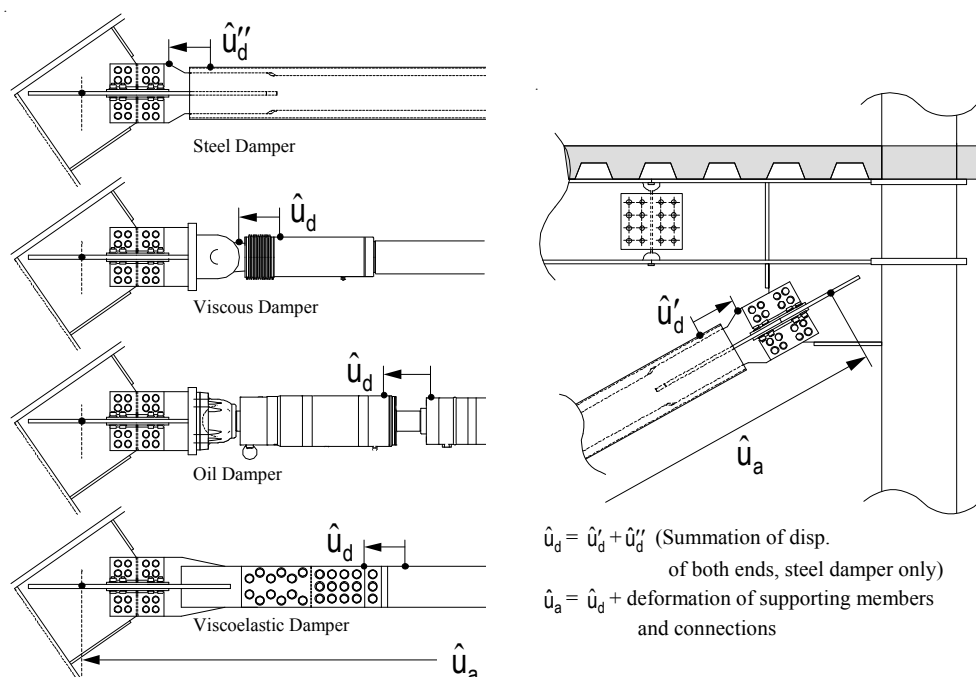


Figure 5 Damper End Conditions and Deformations Recorded

Fig. 5 shows schematically the connection details and deformations measured for the four types of dampers. The steel damper and viscoelastic dampers are rigidly connected the gusset using slip-critical bolts, thus, in addition to the axial force, they can be subjected to bending in- and out-of-plane of the damped bay. In contrast, the viscous damper and oil damper contain universal joints, and they are free from such bending. Axial forces and bending moments in all dampers were recorded by using the strain gages attached. As shown in Fig. 5, the damper stroke and distance change between the diametrically opposite gussets are also measured.

2.2. Test Methods

The number of data channels was about 1,350, the largest among all tests performed previously at E-Defense. Strains in columns, beams, dampers, and other components were measured in order to find all internal forces satisfying equilibrium at every time step. Story drifts, damper deformations, foundation rotations, column rotations, beam rotations, and others were measured to find building local and global deformations. Story accelerations and components accelerations were measured to find inertia forces to both the building and non-structural components.

The JR Takatori ground motion, one of the strongest ground motions recorded during the 1995 Great Hanshin Earthquake was used as the target table motion. The accelerations in all two horizontal and one vertical directions were typically scaled to 15%, 40%, 50%, 70%, and 100% in the order of the test performed. After the damped building tests, the frame without dampers were tested using 5, 20, 40, and 70% Takatori motion. 100% Takatori motion was not applied to the undamped building for the safety reason. In a different project lead by the writer, a full-scale 4-story moment-resisting frame without dampers collapsed at 100%e Takatori motion (Yamada et al. 2009, Suita et al. 2009). Shake table tests of white noise excitation, harmonic vibration, and free vibration were also performed. During the break between the shake table tests, forced vibration tests were conducted by operating two vibrating machines set on the building roof. Ambient vibration was monitored after erection of steel skeleton until all tests ended.

3. TEST RESULTS AND DISCUSSIONS

3.1. Observed Responses

Unless otherwise noted, global and local responses in Y-direction will be considered from now on. For the building with dampers, the displacements were about 1.4 times those in X-direction. Fig. 6 shows damper force and damper stroke for the four types of dampers at 1st story under 15%, 50%, and 100% Takatori motions. As shown by Fig. 6a, the steel damper behaved elastically under 15% Takatori motion, and elasto-plastically under 50% and 100% Takatori motions. In contrast to this deformation-dependent damper, other three damper types in Figs. 6b to d are velocity-dependent, and showed energy dissipation even at 15% Takatori motion, amount of which was large enough against the energy stored (strain) during the smaller shaking. As in Figs. 6b and c, viscous damper and oil damper showed similar hysteresis at large shaking. But the latter showed clearer change of hysteresis shape: it behaved linearly under 15% and 50% Takatori motions, and nonlinearly under 100% Takatori motion due to activation of the relief valve. Viscoelastic damper behaved linearly regardless of shaking intensity (Fig. 6d).

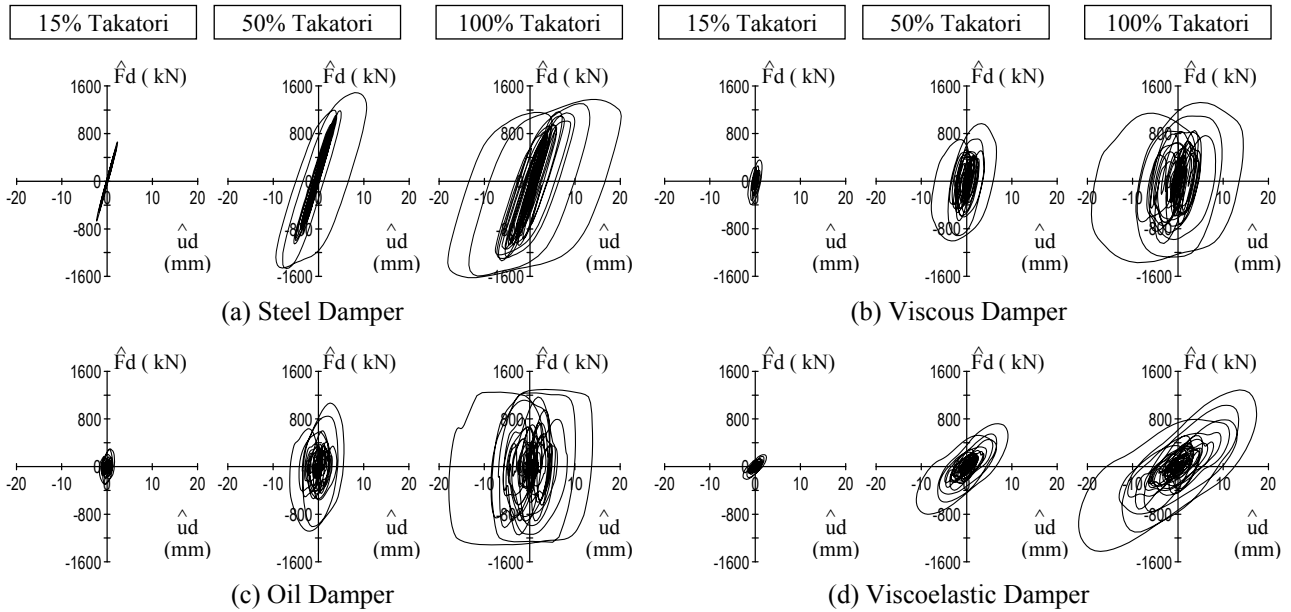


Figure 6 Damper Axial Force and Stroke, Four Types of D3 Dampers at 1st Story (15, 50, and 100% Takatori Motions)

Note also that the steel dampers and viscoelastic dampers in the building were exposed to bending both in-plane and out-of-plane of the frame due to the story drifts in two perpendicular directions, as described earlier. However, the individual damper tests performed at TIT imposing only the same axial deformation showed the forces very close to those recorded during the building test. Thus, it was concluded that bending deformation of the magnitude developed during the building test did not have any detrimental effect against damper performance, which would justify the typical individual damper tests employing idealized boundary conditions free from bending.

Fig. 7 shows peak story shear, story drift angle, and floor acceleration of the building specimen with four types of dampers at 50% and 100% Takatori motion. Fig. 7 also includes the building without dampers, whose responses at 100% Takatori motion are estimated as 2 times those for 50% Takatori motion. This is because test was performed only up to 70% Takatori motion for the undamped building, as mentioned earlier. As shown in Fig. 7, story drift angles of the damped building at 100% Takatori motion are within the design target of 1/100 radian. Peak responses of the building with dampers are considerably less than those without dampers. However, Fig. 7(a) upper row shows relatively high shear and acceleration when using steel dampers, since energy dissipation of steel damper is less than others at smaller shaking, as mentioned (Fig. 6).

3.2. Model Idealization

The 5-story building with dampers can be approximately represented by the spring model such as shown in Fig. 8. The model consists of damper and supporting member (e.g., brace) connected in series, as well as a frame connected to these components. Note that the model behaves like a shear beam, but the cantilever bending deformation mode can be approximately included by tuning the spring representing “brace” (Kasai & Iwasaki 2006a).

The parameters affecting control are the mass, elastic stiffness of the frame and brace, and damping and stiffness of the damper. As a general term, “added component” is defined for the damper and brace connected in series. In this component, the brace

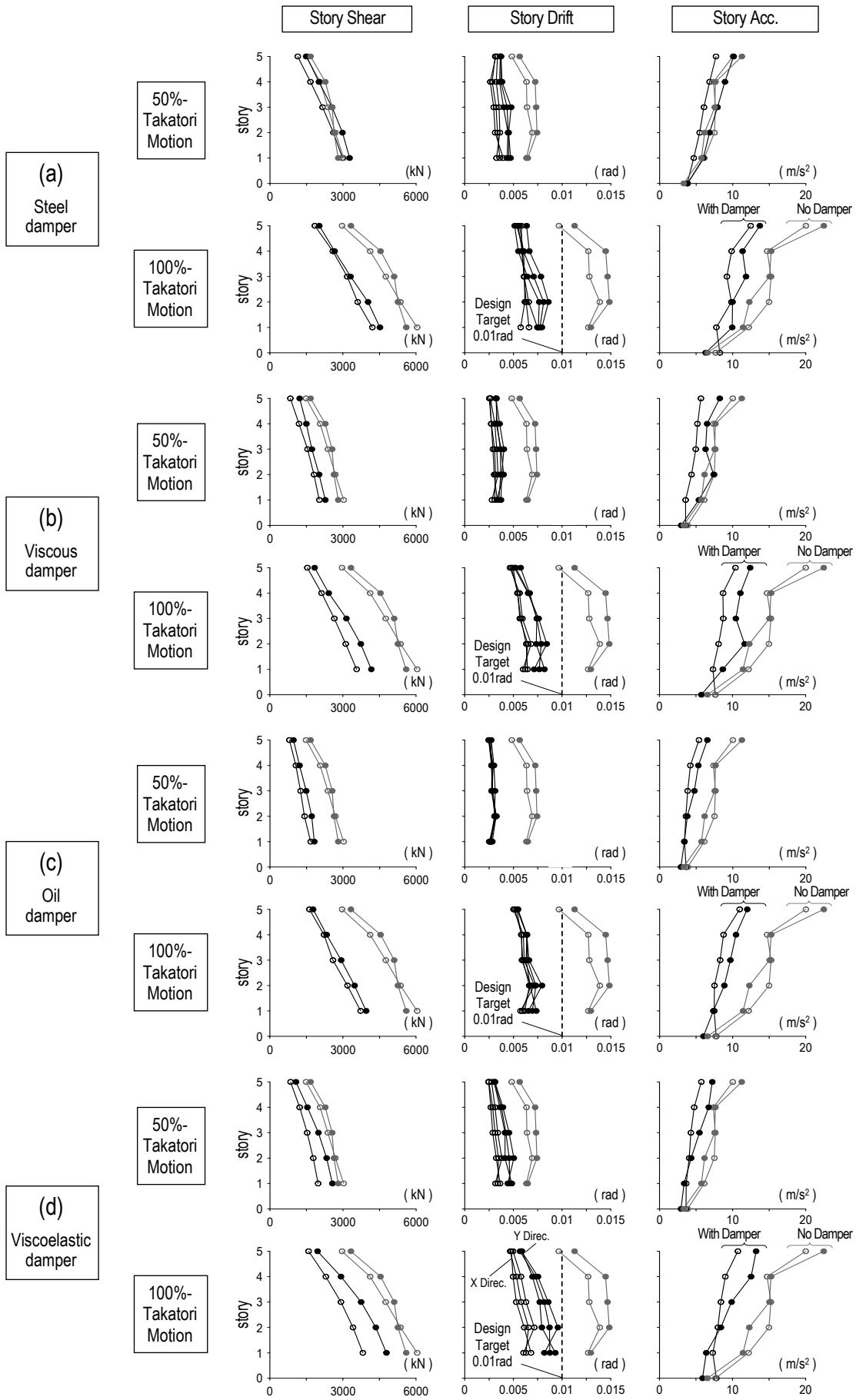


Figure 7 Peak Responses of the Damped and Undamped Buildings (50 & 100% Takatori Motions)

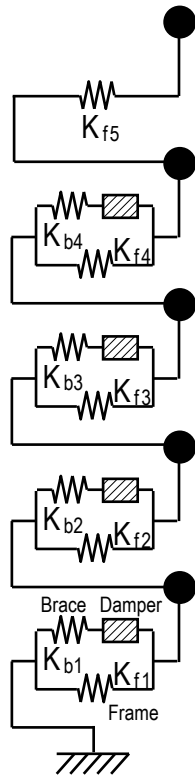


Figure 8 Characterization of the 5-Story Building

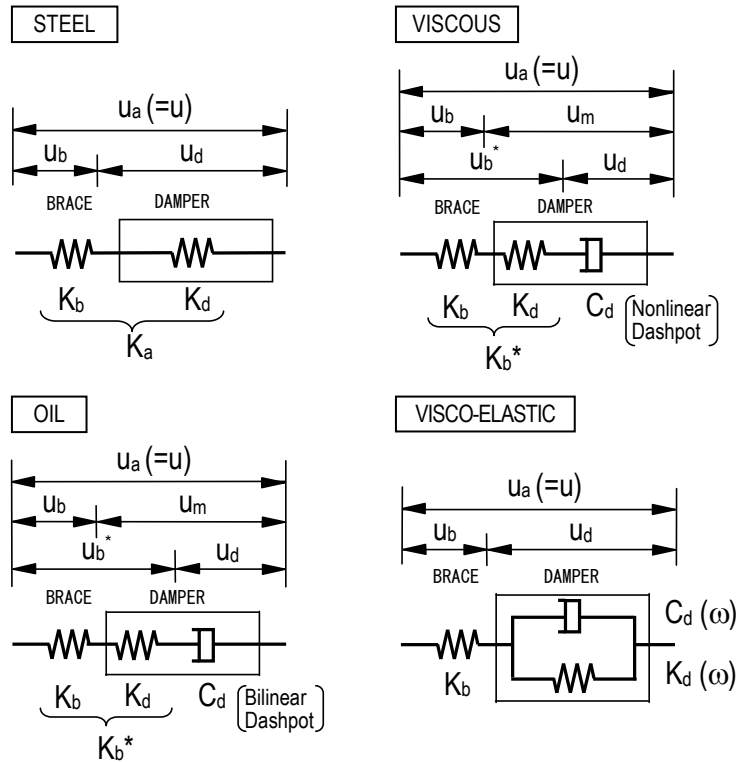


Figure 9 Added Components Containing Dampers

deformation can reduce the damper deformation, and consequently energy dissipation. Fig. 9 shows added components containing different types of dampers. The brace is considered to be elastic and its stiffness is defined as K_b . Following comments are given for each added component:

(a) Energy dissipater of steel damper is expressed by an elasto-plastic spring, and its elastic stiffness and yield force are defined as K_d and F_{dy} , respectively. Added component elastic stiffness K_a is expressed simply by K_d and K_b only.

(b) Energy dissipater of viscous damper is expressed by a nonlinear dashpot. The dashpot force equals the viscous coefficient C_d times the fractional power of the velocity. Like the oil damper, it has elastic stiffness K_d due to compressive modulus of the viscous polymer liquid, and equivalent brace stiffness K_b^* , putting K_d and K_b together, is sometimes used for the ease of modeling.

(c) Energy dissipater of oil damper is expressed by a bilinear dashpot, and its viscous coefficient C_d switches between high and low values when the “relief load” is exceeded. The damper also has elastic stiffness K_d , due to compressive modulus of the oil. Thus, equivalent brace stiffness K_b^* , putting K_d and K_b together, is sometimes used for the ease of modeling.

(d) Energy dissipater of viscoelastic damper is expressed by a dashpot and a spring connected in parallel. Their viscous coefficient C_d and elastic stiffness K_d , respectively, depend on the excitation frequencies. This added component, unlike others, includes parallel elements, and the brace having elastic stiffness K_b is the only element attached in series.

The simplified model such as shown in Fig. 8 is useful for basic supplemental damping design balancing the frame and dampers, theoretical evaluation for dynamic properties of the building with dampers, approximate dynamic time history analysis or equivalent static analysis predicting overall as well as local (damper) responses. Some of these will be demonstrated in Secs. 3.3 to 3.5.

3.3. Equivalent Linearization to Evaluate Dynamic Properties and Peak Responses

Fig. 8 shows hysteresis curves of the energy dissipater, added component, and system (including frame), for the cases using four different dampers. Sinusoidal deformation of a given peak deformation magnitude is imposed to each, and the figure plots the steady-state responses. Note the black dot (●) indicating the point of peak deformation, where the “storage stiffness”, or so-called equivalent stiffness, is defined as the corresponding force divided by the deformation. Likewise, “loss stiffness” is defined as the force at the white dot (○) divided by the peak deformation. From now on, the storage stiffness K_d' , K_a' , and K' , the loss stiffness K_d'' , K_a'' , and K'' will be considered for the energy dissipater, added component, and system, respectively.

According to Figs. 9 and 10, the storage and loss stiffnesses are mathematically expressed for the damper, using its properties such as K_d , C_d , F_{dy} , excitation frequencies, and deformation amplitudes, depending on damper type. The storage and loss stiffnesses of the added component are then evaluated by additionally involving the brace stiffness K_b , and those of the system by involving the frame stiffness K_f . Based on these, one can determine the forces at the peak and zero displacements, respectively, and subsequently the peak force, energy dissipated, deformation lag and magnitudes at each component, making evaluation of the control system possible. The writers proposed such methods for all types of dampers mentioned above (Kasai et al. 2005, 2006b, 2007 and 2008a).

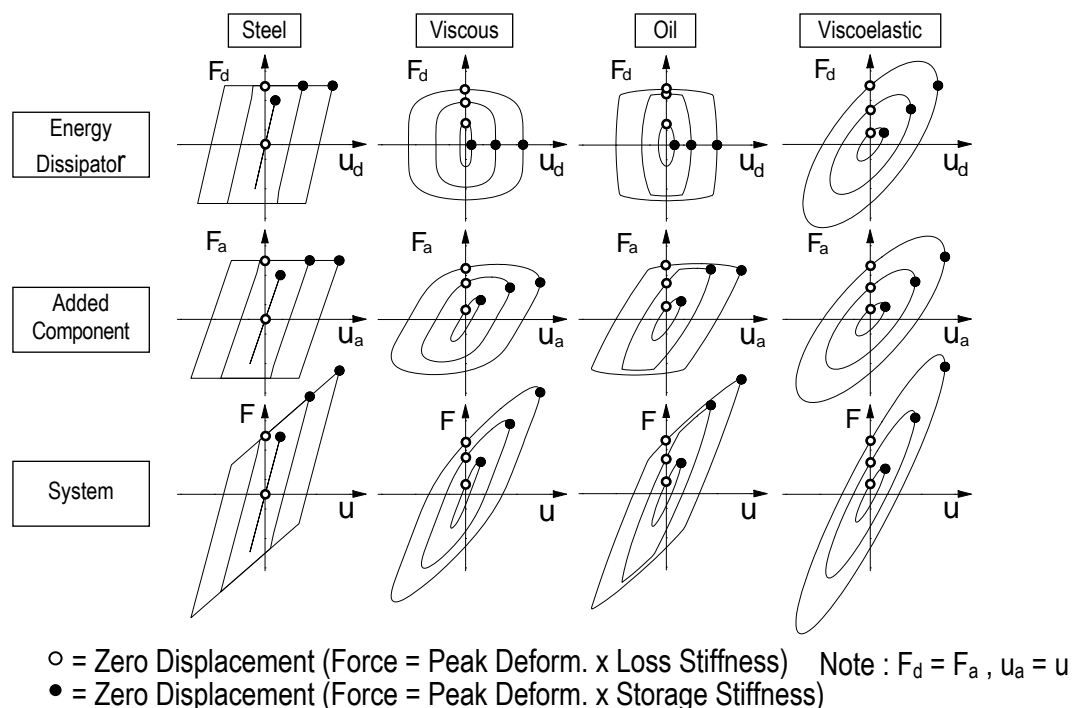


Figure 10 Steady-State Responses of Energy Dissipaters, Added Components, and Systems for 4 Different Dampers

Fig. 11 shows such evaluations for the 1st and 4th stories of the 5-story building at the story drift angles due to several different input scales of the Takatori motion. It shows the peak horizontal shear force of the damper, frame, and combined system, as well as shear forces of the damper and combined system at the instance of peak roof displacement.

Evaluations are pursued in the following order: The damper properties are estimated using the results of the writers' detailed harmonic loading tests for the same damper and cross referencing with the data provided by the damper manufacturer. The brace stiffness K_b is estimated by considering the measured damper force and the difference between the measured story drift and horizontal component of the damper stroke during the shake table tests. Likewise, the frame stiffness K_f is also estimated by considering the measured story shear force and the story drift.

As shown by Fig. 11, remarkable correlations between the evaluated value and test results are obtained, and the effects of different hysteretic characteristics of the

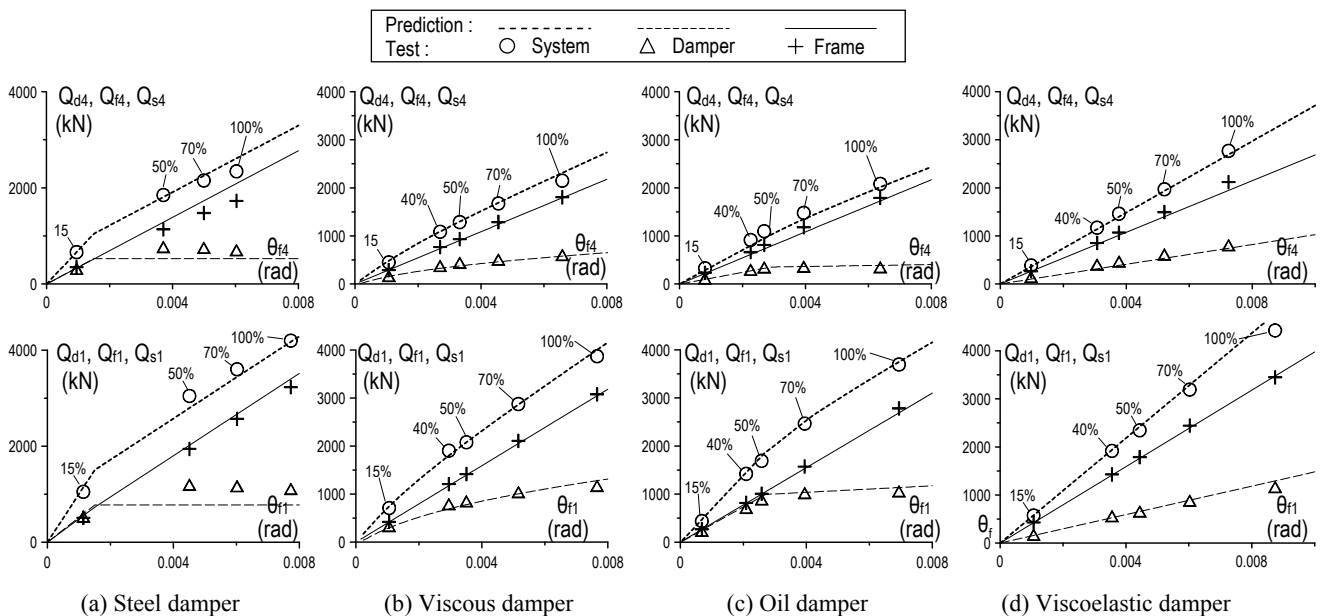


Figure 11 Peak Shear Forces and Shear Forces at Peak Roof Displacement: Forces of Damper, Frame, and Combined System (Q_{di} , Q_{fi} , and Q_{si}) at 4th and 1st Stories ($i = 4$ and 1) Levels

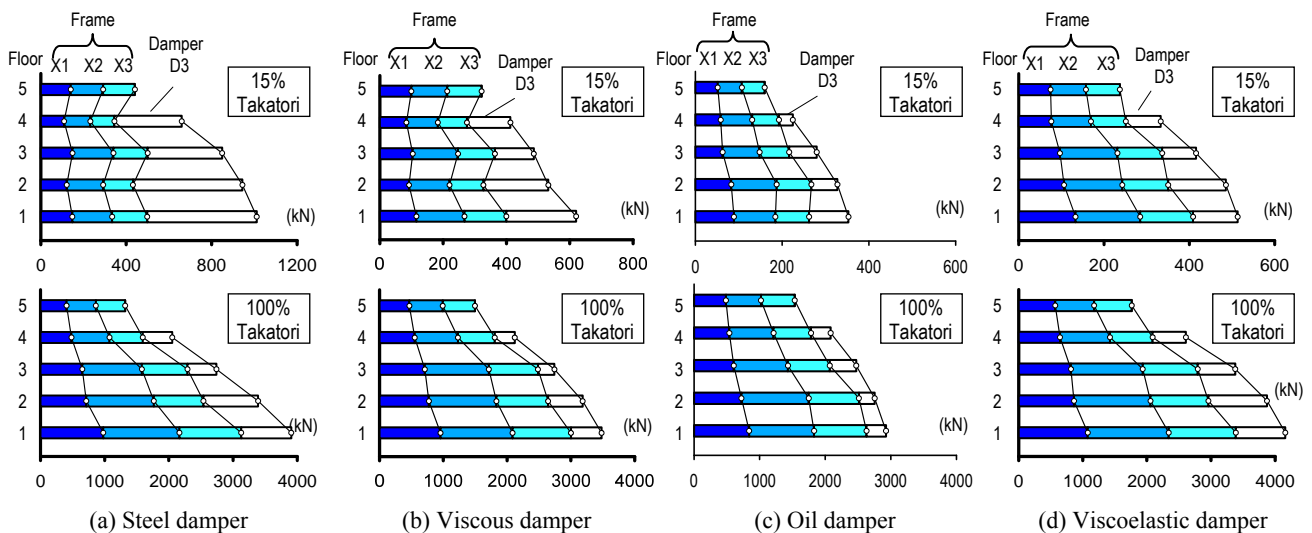


Figure 12 Shear Force Distributions for Each Frame and Damper at Peak Roof Displacement

dampers on the peak force of the dampers, added components, and systems are conveniently expressed by the method. According to Fig. 11, it can be said that the diagrams constructed using the theoretical relationship of harmonic force and deformation for the damper, brace, and frame are consistent with the results from random shaking tests using various levels of the Takatori motion. Accordingly, the balance of seismic forces between the damper and frame can be estimated in a simple manner by using the theoretical relationship between them. Theoretical estimates are possible for peak forces, or forces at any selected instance, if the damper properties, brace stiffness, and frame stiffness, and vibration period are given.

The steel and viscous dampers tend to attract large forces at relatively smaller shaking by the 15% Takatori motion (Figs. 11 and 12), because the former is elastic and the latter produces relatively large damping force at low velocity due to its nonlinearity. Fig. 12 shows the force distributions to the three parallel frames in Y-direction, where they are about proportional to horizontal stiffness of the frames, as expected. For the two types of dampers mentioned above, relatively large transfer of column forces at 5th and 3rd story to the damped bay of immediately lower stories occurs via floor slab at 15% Takatori motion. These are because 5th story has no dampers and 3rd story has considerable smaller dampers compared with the 2nd story.

Note also the distributions can vary considerably from those plotted in Fig. 12 at different instances. For example the instances of peak damper forces show much larger share by the dampers than the frame, especially for the dampers having large phase angle between the force and deformation.

3.4. Response and Design Evaluation Using Performance Curves

Using mathematical expressions for the storage stiffness and loss stiffness mentioned in the previous section, the effective vibration period and damping ratio of the building with dampers can be evaluated theoretically. Using these and idealized seismic response spectra, seismic peak responses of systems and local members can be expressed by a continuous function of the structural and seismic parameters. The curves plotting the functions have been called as “performance curve”, which promotes understanding of the commonalities and differences between various systems having distinct energy dissipation mechanisms. It requires only simple calculations, and its prediction agreed well with the results of the extensive numerical experiments (Kasai et al. 2005, 2006b, 2007 and 2008a).

Since publication of performance curves for steel dampers and viscoelastic dampers (Kasai et al. 1998, Fu & Kasai 1998), the concept and methods have been confirmed by many parties and expanded to include more factors such as higher mode vibrations, yielding as well as different hysteretic characteristics of frames, and many other damper types (e.g., Kasai et al. 2005, 2006b, 2007 and 2008a). To-date, the performance curves have been adopted by more than six different design specifications in Japan, covering response control of steel frames, reinforced-concrete frames, and timber frames.

Fig. 13 shows y-direction pseudo-velocity response spectrum with 2% damping ratio, and considering the range of vibration periods of the 5-story building with different dampers and that without dampers, constant pseudo-velocity spectrum of 162 cm/s is considered to represent the input table motion (Fig. 13). Note that the original Takatori NS and EW records were applied in the axes rotated 135o counter-clockwise from building's x- and y-directions, respectively, and the spectrum is produced

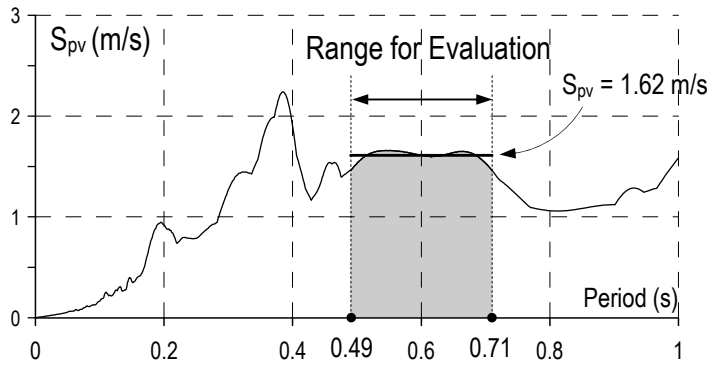


Figure 13 Pseudo-Velocity Spectrum of 100% Takatori Motion (Y-Direc. Damping Ratio 0.02)

accordingly. The pseudo-velocity y-direction is about 1.4 times that of x-direction, and is about 1.1 times that of the so-called BCJ-L2 showing constant pseudo-velocity of 148 cm/s at 2% damping ratio.

The above-mentioned constant spectral value is combined with effective periods and damping ratios of the damped 5-story buildings, and the spectral responses shown in Fig. 14: the curves show both displacement reduction ratio R_d and force (or acceleration) reduction ratio R_a , the values of the peak responses normalized to those having no dampers. The role of the balance among the frame, damper, and supporting member is summarized below for each damper type:

(a) When using steel dampers, K_d/K_f and μ govern the response reduction. The former is a ratio of the added component elastic stiffness to the frame elastic stiffness, and the latter is a ductility ratio of the system and equally the added component.

(b) When using oil dampers, K_{d1}''/K_f and K_b/K_f govern the response reduction. The former is a ratio of the dissipater loss stiffness (defined when peak force is below the

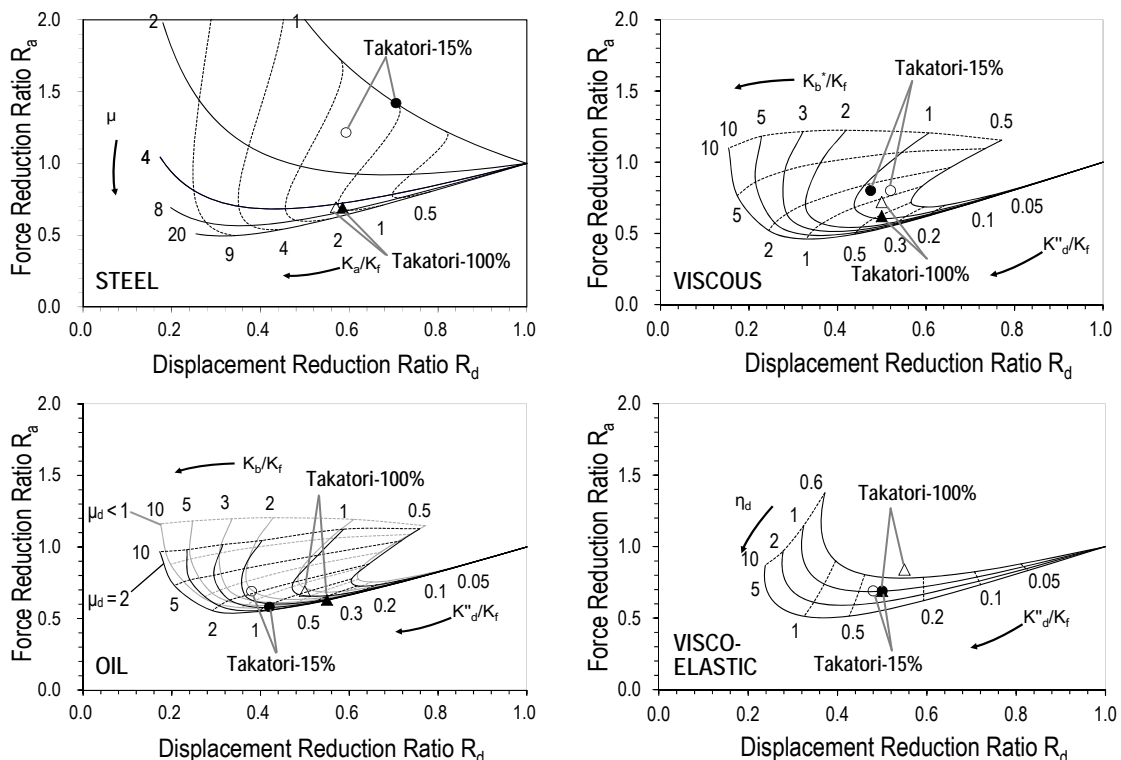


Figure 14 Control Performance Comparison between Test Results and Evaluations by Performance Curves (White Symbols: Test Results, Black Symbols: Predictions)

relief load) to the frame elastic stiffness, and the latter is a ratio of the brace elastic stiffness to the frame elastic stiffness. Relief load of the dissipater is already set optimum in the curves.

(c) When using viscoelastic dampers, K_d''/K_f and K_b/K_f govern the response reduction. The former is a ratio of the dissipater loss stiffness to the frame elastic stiffness, and the latter is a ratio of the brace elastic stiffness to the frame elastic stiffness.

(d) When using viscous dampers, K_d''/K_f and K_b^*/K_f govern the response reduction. The former is a ratio of the dissipater loss stiffness to the frame elastic stiffness, and the latter is a ratio of the equivalent spring stiffness to the frame elastic stiffness. The equivalent spring stiffness is obtained from the damper elastic stiffness and brace elastic stiffness (Fig. 9).

Fig. 14 enables the users to quickly evaluate response reduction: To a certain extent, larger damper leads to more reduction of displacement and force. However, excessively large damper appears to be ineffective for displacement control, and detrimental in force control, as observed from sharply rising curves. Fig. 14 also shows decrease of control effectiveness by smaller brace stiffness: brace deforms more, and damper deformation as well as energy dissipation becomes smaller.

In the specifications and related papers, the performance curve is typically used to determine the required amount of damper capacities to satisfy the target drift. Instead, the present paper evaluates damped 5-story building, comparing with the undamped building and interpreting the effect of damper, brace, and frame by the use of the performance curve.

Using the deformations of damper and added component obtained from the test, the storage and loss stiffnesses of the added components are estimated. Estimating each stiffness (e.g., K_a , K_d'' , and K_f) appearing in Fig. 14 as the sum of the corresponding stiffnesses from 1st to 5th story levels, the stiffness ratio (e.g., K_a/K_f and K_d''/K_f) is determined and plotted by black symbol in Fig. 14. As will be explained in Sec. 3.5, except for the other tests, the first test series conducted using the steel dampers showed about 1.3 times stiffness for the frame, and such K_f value is considered for the steel damper case. Note also that the brace stiffness at each story is obtained by taking the ratio between the damper force and difference of story drift and horizontal component of damper deformation, and it is divided by the frame stiffness to obtain the brace stiffness ratio. Average of the ratio from 1st to 4th story level is considered as the ratio K_b/K_f for Fig. 14.

As for the test results, the story drift ratios are averaged first and its value and base shear force are compared with those of undamped building, and response reduction ratio plotted by the white symbol in Fig. 14. The black and white symbols are close, which would justify interpretation of control effectiveness using the performance curve. Fig. 14 indicates very similar and excellent performance for the four dampers at 100% Takatori motion. Relatively large accelerations and base shear are clearly observed in case of steel dampers at 15% Takatori motion. In the viscous damper case, control is less effective at 15% Takatori motion probably due to reasons described in Sec. 3.5, but it appears to be still good overall. In the oil damper case, the performance at 15% Takatori motion is more effective due to linear viscous response maximizing energy dissipation (set up to the level of 50% Takatori), and shows excellent damping effect in all level of excitation. Note, however, that oversizing of the damper exceeding the required capacity was more prominent than

other dampers due to less available choices. In the viscoelastic damper case, the performance is expected to be almost independent of the excitation level due to the linear behavior, but less effectiveness at 100% Takatori motion is observed from the test, which is being investigated by the writer.

3.5. Dynamic Properties of the Building Specimens

In order to investigate the effect of beam composite action on the stiffness of the frame, cracks on all concrete floors and roof were recorded. This was also compared with the shifting of the neutral axis estimated from the strain gages attached to all beams. Cracks formed when the story drift reached approximately 1/200 rad. and significantly increased after the test with steel damper using 100% Takatori motion, and the final test without dampers using 70% Takatori motion. In the first test series conducted using steel dampers, the stiffness was about 1.3 times stiffness for the frame with other dampers. Also, during a test series of each damper, the frame stiffness was the largest and lost about 10 to 15% at the end of the series. The cracks of floor slabs are recognized to correlate with this change. Importantly, moment of inertia of the composite beams compared with the bare steel beams were typically two to three times at positive bending and up to two times at negative bending even after the many tests performed.

Table 2 lists the 1st mode vibration periods and damping ratios obtained for all the tests. The small, medium, large, and catastrophic shaking levels indicated in Table 2 means, 15, 40, 70, and 100% Takatori motion for the building with dampers, and 5, 20, 40, and 70% Takatori motion for that without dampers. The building with steel dampers shows shortest period and smallest damping ratio, consistent with the observations from Figs. 6 and 7. However, they become longer and larger, respectively at larger shaking, resulting in control of both acceleration and displacement. The building with oil dampers showed the largest damping ratio of about 17% and the smallest responses (Fig. 7c). But this is mostly due to over-sizing in damper size, as explained in Sec. 3.4. The building with either viscous dampers or viscoelastic dampers showed damping ratios of up to 10%, and performed well (Fig. 7).

The present paper uses only basic system identification results using real modes and considering effects of inevitable table rocking motions. In spite of different nonlinear behaviour of the dampers and the building, the linear identification method (Kasai et al. 2011b) assuming real vibration mode still produced excellent results. Note,

Table 2 First Mode Damping Ratio and Vibration Period

Shaking Level		X-Direction				Y-Direction			
		Small	Medium	Large	Catastrophic	Small	Medium	Large	Catastrophic
h_1	Steel	0.014	0.031	0.057	0.084	0.020	0.060	0.061	0.100
	Viscous	0.043	0.117	0.105	0.137	0.066	0.096	0.123	0.138
	Oil	0.223	0.206	0.201	0.226	0.187	0.190	0.180	0.172
	Viscoelastic	0.097	0.101	0.096	0.103	0.115	0.090	0.092	0.100
	No Damper	0.010	0.013	0.010	0.021	0.011	0.013	0.011	0.014
T_1 (sec)	Steel	0.469	0.482	0.494	0.518	0.487	0.516	0.554	0.562
	Viscous	0.536	0.540	0.549	0.557	0.575	0.576	0.590	0.612
	Oil	0.555	0.541	0.536	0.546	0.586	0.599	0.617	0.632
	Viscoelastic	0.578	0.575	0.591	0.596	0.630	0.615	0.613	0.616
	No Damper	0.650	0.672	0.670	0.650	0.705	0.708	0.703	0.710

Note : h_1, T_1 = 1st mode damping ratio and vibration period

however, the method could not estimate the properties in the 2nd mode and higher for the case of steel dampers that exhibits most significant variation of the stiffness during vibration. The method showed less accuracy for the frame without dampers at the 70% Takatori motion, probably due to yielding of the members and connections of the building

4. RESPONSES DURING THE 2011 TOHOKU-OKI EARTHQUAKE

4.1. The Tohoku-Oki Earthquake

At 14:46 on March 11, 2011, the Tohoku-Oki Earthquake of magnitude 9.0 occurred off Sanriku coast of Japan. It caused tremendous tsunami hazard in the pacific coast of eastern Japan, killing more than 15,000 people, destroying and washing away cities. Where ground acceleration was large, except for some areas of soft ground, the response spectrum indicates short dominant period, which was probably the main reason for relatively small seismic damage. On the other hand, Tokyo relatively far from the epicenter was subjected to the ground motion of short to long period components, and the recorded accelerations were the largest than ever in Tokyo area.

As the important reconnaissance effort of Japan Society of Seismic Isolation (JSSI), the writer and collaborators investigated performance of supplementally-damped buildings (Kasai et al. 2013). Since no damage was found from such buildings, acceleration records of many supplementally-damped buildings and conventional buildings were studied and compared. The following sections highlight some of the findings.

4.2. Buildings Considered and Data Analysis Scheme

In this paper, 29-story conventional building, and 21, 37, 38, 41, and 54-story supplementally-damped buildings, all located in Tokyo, will be explained. The peak accelerations at the building base ranged from 71 to 142 cm/s^2 , and those at top of the building ranged from 118 to 316 cm/s^2 . The average story drift angle (ratio of peak displacement of top to its height) varied from 0.0010 to 0.0030 rad.

As explained earlier (Kasai et al. 2012c, 2013), many of the ground motion records in Tokyo showed the spectral velocity almost uniform for the vibration periods from 0.5s and 20s, and its magnitude exceeded even the largest spectral value due to the 2004 Niigata Chuetsu Earthquake that concentrated at the period about 7s. Thus, unlike the responses during the 2004 Niigata Chuetsu Earthquake, the responses of the tall buildings in Tokyo were dominated by not only the shorter period motions but also the long period motion.

Displacements of the structure are calculated from the recorded accelerations by using two methods. The results are compared with each other in order to confirm their reliability (Kasai, 2011c). Method 1 performs double integration together with hi-pass filtering in frequency domain. The cut-off frequency is typically 0.05 or 0.1Hz. Method 2 first obtains modal properties such as vibration period, damping ratio, and participation vector, by applying the basic system identification technique explained in Sec. 3.5. Then, the time histories of acceleration and displacements are obtained for each mode using the base acceleration recorded, and they are superposed to obtain acceleration and displacement. As will be demonstrated, the displacements from method 2 agreed well with those from method 1, and accelerations from method 2

agreed with those recorded. Thus, calculated modal properties would be adequate and the buildings must also have behaved linearly.

4.3. Tall Building without Dampers

The building is a seismically-resistant 29-story steel building constructed in 1989 (Hisada et al. 2011, 2012, Kasai et al. 2012c). It is a school building of Kogakuin University, located in Shinjuku ward of central Tokyo. The building height is 143 m, and floor plan dimension is 38.4 and 25.6 m in EW and NS (x- and y-) directions, respectively (Hisada et al. 2011, 2012, Kasai et al. 2012c).

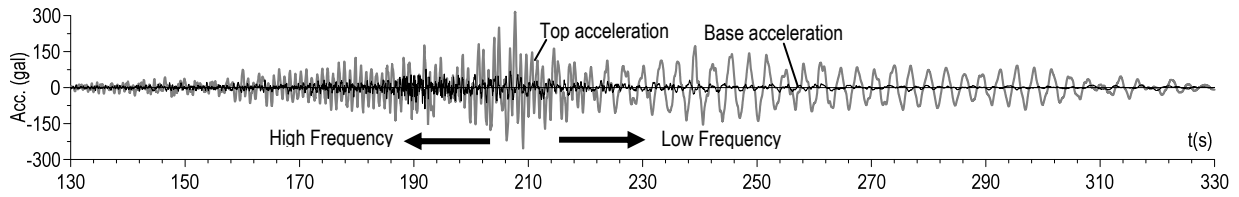
The peak accelerations in x- and y-directions were 91 and 89 cm/s^2 at the base, and 235 and 316 cm/s^2 at the top floor, respectively. The average drift angle is 0.029 rad., and the structure remained elastic. The vibration periods for the first three modes are 2.96s, 1.00s, and 0.52s for x-direction, and 3.10s, 0.94s, and 0.47s for y-direction, respectively. Likewise, damping ratios are 0.017, 0.018, and 0.034 for x-direction, and 0.021, 0.016, and 0.034 for y-direction, respectively. Damping ratio 0.01 was estimated from small amplitude vibration tests before 2011 (Hisada 2011).

Fig. 15a compares acceleration records at top floor and base in y-direction. The earthquake duration is long, and is considered to be about 200 seconds. For the first 90 seconds of the figure, high frequency response of the top floor is apparent, as confirmed by the large number of cycles per unit time. These are caused by the high-frequency ground shaking, as shown by the base accelerations. In contrast, for the last 110 seconds, low frequency response dominated. The ground shaking was weak (Fig. 15a), but its low frequency contents excited the first mode of the building.

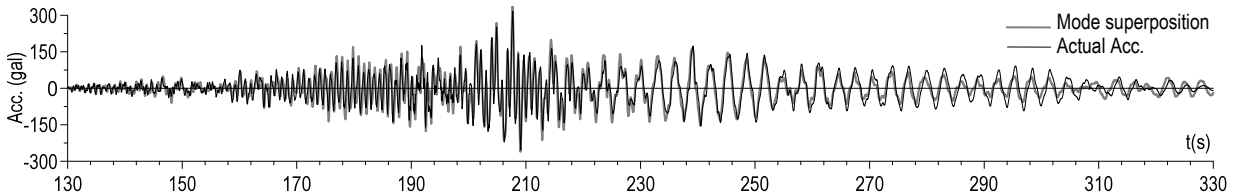
Fig. 15b compares the top floor acceleration recorded with that calculated by method 2 (Sec. 4.2). Fig. 15c compares relative displacement of top floor obtained by double integration of the record (method 1) with that calculated by method 2. In some cycles the peak values by the both methods differ a little, but the displacements agree well overall. The good agreement between responses calculated from completely different schemes would suggest not only accuracy of the calculated modal properties but also the reliability of the records.

Fig. 16a shows the acceleration of each mode at the top floor. As mentioned earlier, it is dominated by the 2nd, 1st, and 3rd modes in the order of weight for the first 90 seconds. For the later 110 seconds, the 1st mode response increases and become dominant, with slight contribution from the 2nd mode. As Fig. 16b shows, for the 16th floor the 2nd mode is much more dominant, developing almost the same acceleration as top floor. As for the displacement at top floor (Fig. 16c), the 1st mode dominates throughout the entire duration.

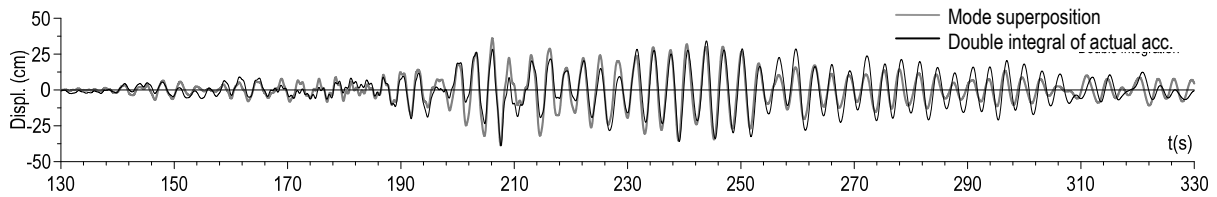
In this manner, what mode governs depends on the type of component and the story level affecting participation vector of vibration. Hisada et al. (2011, 2012) reported moving of furniture, copy machines and others, and falling of ceiling and books. They must have occurred due to large floor accelerations of different frequency contents, respectively.



(a) Accelerations Recorded at Top and Base.

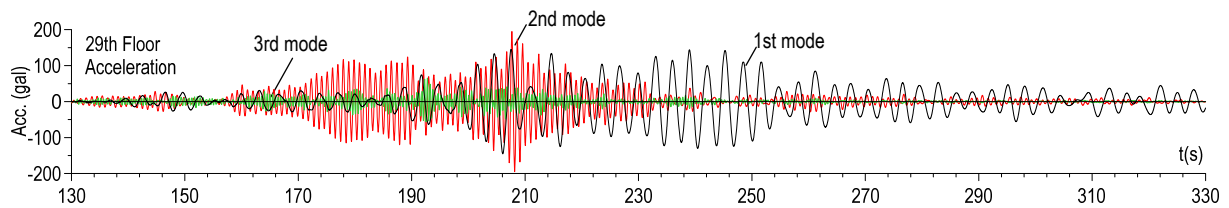


(b) Comparison: Acceleration Obtained by Mode Superposition vs. Actual Recorded Acceleration.

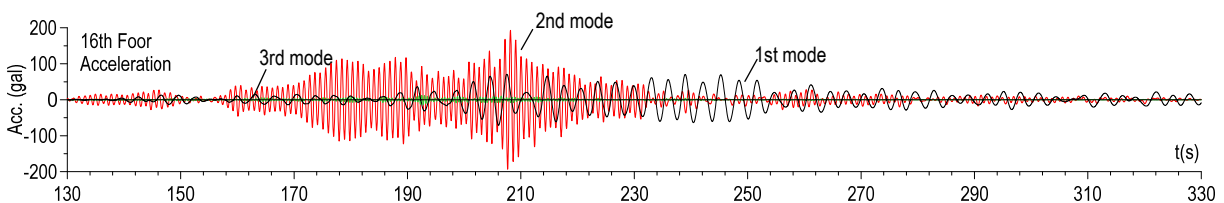


(c) Comparison: Dispt. Obtained by Mode Superposition vs. Double Integral of Recorded Acceleration.

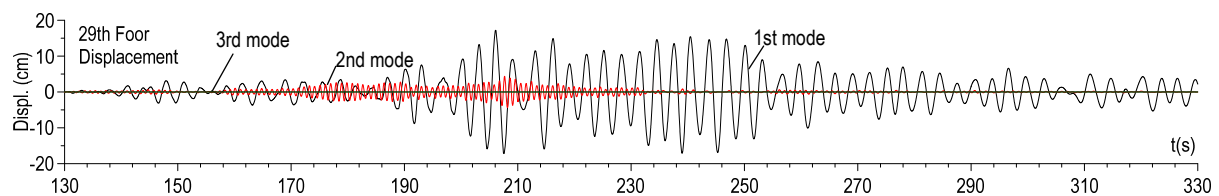
Figure 15 Recorded Accelerations, Double Integration, and Mode Superposition Analysis



(a) Modal Contributions to Top Floor Acceleration.



(b) Modal Contributions to 16th Floor Acceleration.



(c) Modal Contributions to Top Floor Ddisplacement.

Figure 16 Modal Contributions to Acc. and Disp.t of 29-Story Undamped Building

4.4. Deformation-Dependent and Velocity-Dependent Dampers

One of the deformation-dependent damper types, a steel damper is the most inexpensive and most widely used in Japan. During the 2011 Tohoku-Oki Earthquake, the steel dampers in the buildings in Tokyo were either elastic or slightly yielding for the level of the ground shaking. Thus, the building using the steel dampers behaved

like a conventional building, showing little damping and producing more acceleration compared with the buildings with the velocity-dependent dampers. The trend is consistent with that observed from the lab tests (Sec. 3.1, Fig. 6).

Fig. 17 shows the transfer function obtained using the acceleration of building top floor and base for the 38-story building having steel dampers only (Fig. 17a), and the building having both steel dampers and viscous dampers (Fig. 17b). They are located nearby, and were subjected to almost the same ground shaking. The former shows the 1st mode damping ratio of 0.017, similar to the value obtained from the 29-story conventional building explained in Sec. 4.1. On the other hand, the latter showed the 1st mode damping ratio of 0.046.

The larger damping ratio of the building with steel and viscous dampers can be understood from wider resonance curves (Figs. 17a, b). The damping ratio of 0.046, however, is not as large as the one observed from the 5-story building tested (Chapters 2 and 3). Nevertheless, the amount of dampers and viscosity coefficients added were considerable, and still show good vibration control, as will be demonstrated in the subsequent sections.

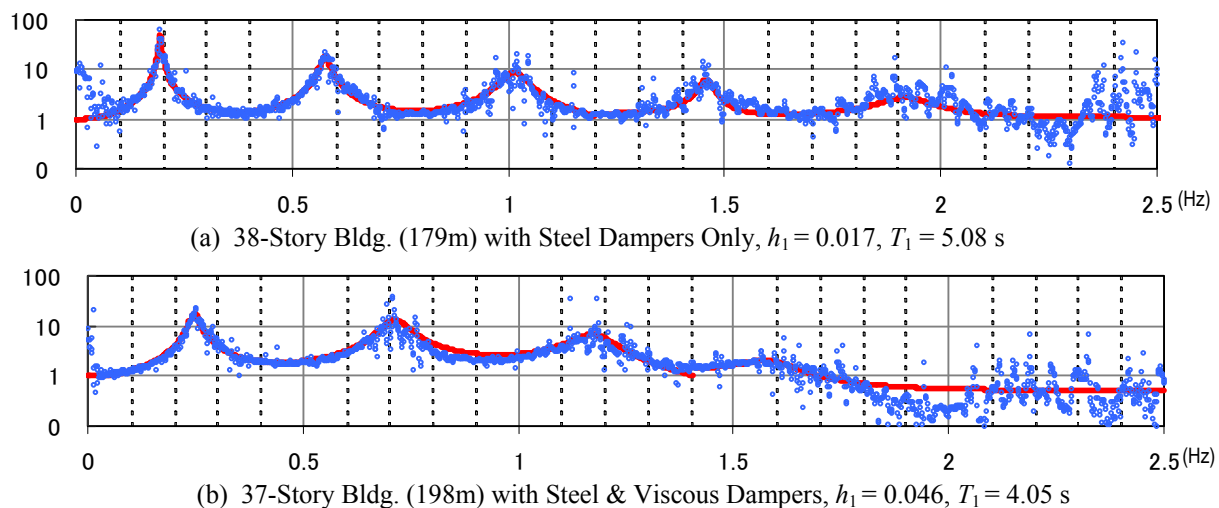


Figure 17 Transfer Functions of Tall Buildings
(a) with Steel Dampers Only, and (b) with Steel and Viscous Dampers

4.5. Tall Buildings with Velocity-Dependent Dampers

Three tall buildings with velocity-dependent dampers will be discussed. They are 21, 41, and 54-story buildings as shown in Fig. 18. Their descriptions will follow:

The first building is a 21-story government office building (Koyoma and Kashima 2011, Kasai 2011c, d, Kasai et al. 2012c). It consists of a steel frame and 336 low yield point steel (wall) dampers and 284 viscous (wall) dampers (Fig. 18a). As found from the full-scale test mentioned earlier, a contrasting case of using only steel dampers lead to large accelerations, since the dampers remained elastic for the level of shaking in Tokyo (Kasai 2011c,d, Kasai et al. 2012c). The 21-story building had been designed to avoid such a situation, expecting that viscous damper would dissipate energy from a small earthquake, and steel damper, the most economical among all types, would dissipate considerable amount of energy at a large quake, respectively.

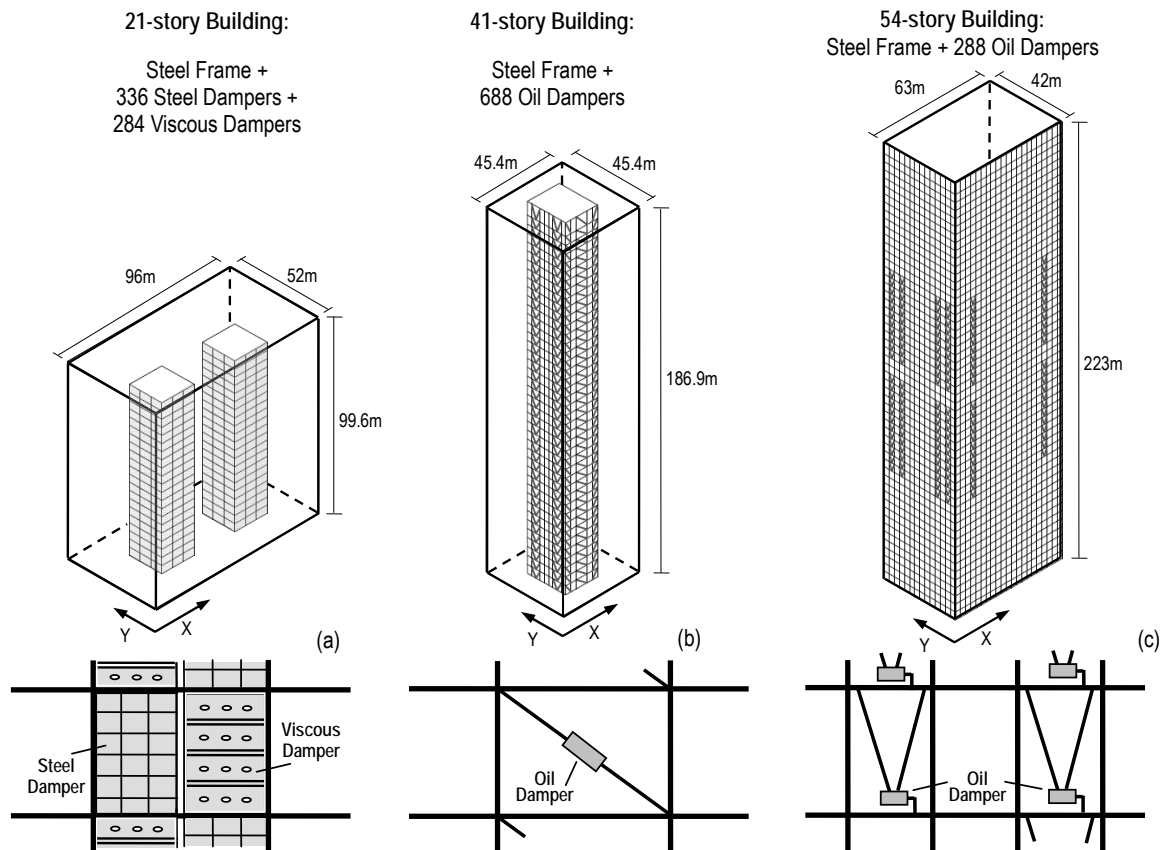


Figure 18 Three Response-Controlled Buildings and Dampers

The second building is a 41-story office building (Kasai 2011c,d, Kasai et al. 2012c). It consists of a frame using concrete-filled tube columns and steel beams, and 688 oil dampers (Fig. 18b) mentioned earlier. The relief mechanism to limit the force was provided, but most likely relief did not occur for the level of shaking.

The third building is a 54-story office steel building constructed in 1979. It was retrofitted in 2009 (Maseki et al. 2011, Kasai et al. 2011c,d) by attaching 288 oil dampers (Fig. 18c). 12 dampers per floor were attached to middle 24 stories of the building. The oil damper is similar to those used for Building 6, except that its relief mechanism is modified to reduce forces near peak responses. This aims to reduce the axial force of the column transmitting the damper force, and consequently uplift force of foundation. Most likely, however, the relief did not occur for the level of shaking.

The ratio of accelerations of top to base will be named as “acceleration amplification ratio”. The largest ratio of both x- and y-directions was 1.80, 2.38, and 2.51 for the 21, 41, and 54-story buildings, respectively. They are well below the ratio of 3.55 obtained in the conventional 29-story building (Sec. 4.3). The three buildings remained elastic, and modal properties are obtained from method 2, and estimated 1st mode damping ratios are about 4%, and those of the 2nd and 3rd modes are almost equal or larger. The 1st mode vibration periods in x- and y-directions are 1.83s and 1.97s for the 21-story building, 3.97s and 4.10s for the 41-story building, and 5.37s and 6.43s for the 54-story building.

Modal properties were estimated for the three buildings, and their accelerations and displacements are obtained from superposition up to the 3rd mode, and accuracies are confirmed to be even better than those shown in Figs. 15b and c shown earlier. Such responses at top floor are shown by black lines in Fig. 19, 20, and 21 for 21-, 41- and 54-story buildings, respectively.

In these three buildings, the acceleration (Figs. 19 to 21) is dominated by the 2nd and 3rd modes for about 100 seconds, and by the 1st mode for later 200 seconds. Whereas, the displacement (Figs. 19 to 21) is dominated by the 1st mode throughout the shaking.

This trend is like that of seismically-resistant 29-story building, but the amplitudes are believed to be smaller due to the supplemental damping. Thus, the responses are compared with those of lower but possible damping ratio representing a hypothetical case of not using the dampers. The modal period is unchanged, assuming small stiffness of the damper. The 1st to 3rd mode damping ratios are uniformly set to 1% and superposition is repeated. The results are shown by gray lines in Figs. 19, 20, and 21 for 21-, 41- and 54-story buildings, respectively.

In all the three buildings, their responses are considerably smaller (black lines) than those with low damping (gray line). The peak accelerations and displacements are

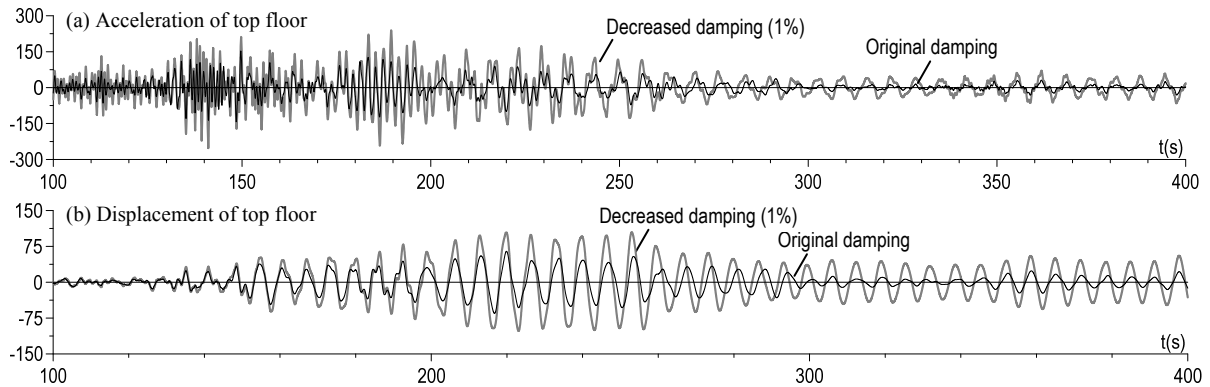


Figure 19 21-story Building with Different Damping Ratios (y-dir.).

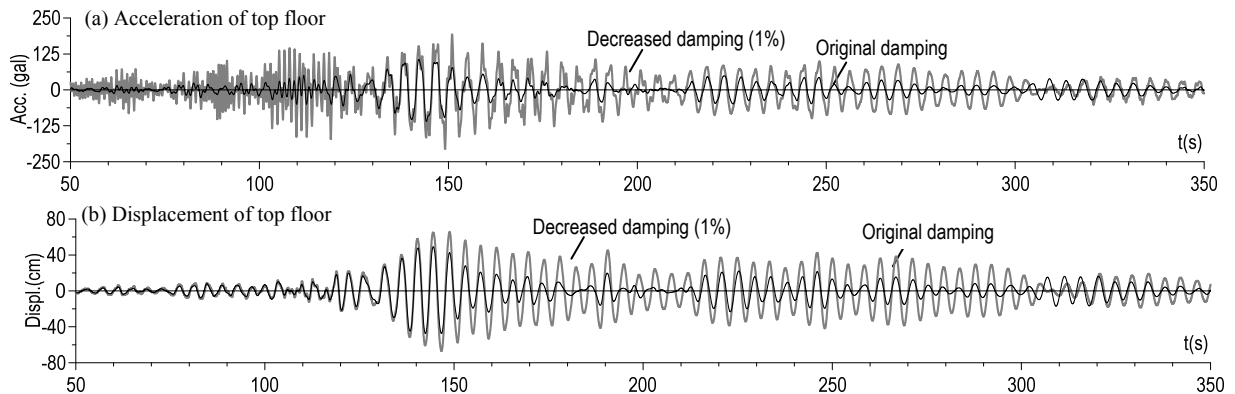


Figure 20 41-story Building with Different Damping Ratios (x-dir.).

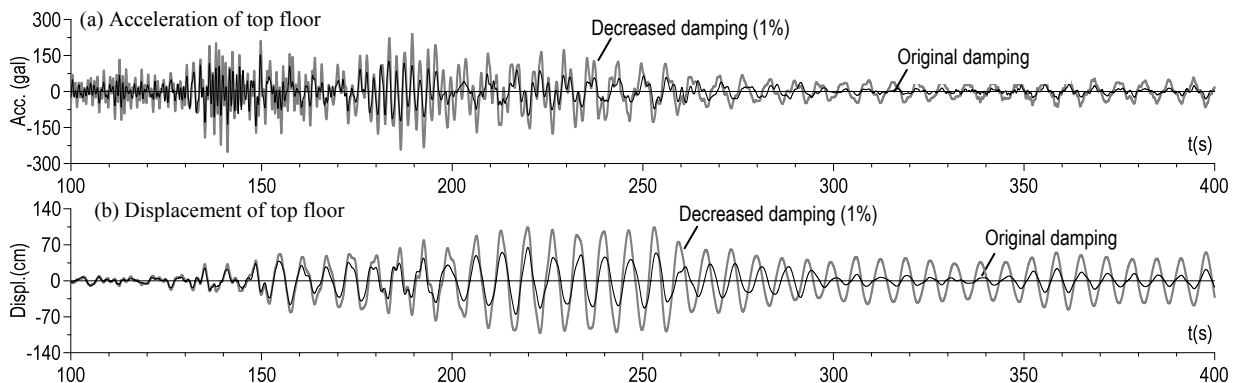


Figure 21 54-Story Building with Different Damping Ratios (y-dir.).

about 0.5 and 0.7 times those of the low damping case. Moreover, between significant ground shakings, the responses decay much faster, and number of large cycles is reduced considerably. These help reducing damage and fatigue of structural and non-structural component as well as fear or discomfort of the occupants. In order to quantify such an effect, root mean square of the acceleration and displacement at top are calculated, and their values appear to be about 0.4 and 0.5 times those with low damping, respectively.

4.6. Component Responses in Controlled Building

Inertia forces against structural and non-structural components including equipment and building content are produced by accelerations in the building. Large accelerations typically developed at upper stories cause falling, overturning, shifting, crashing, rupture, and excessive vibration of a variety of non-structural components.

As a matter of fact, economic loss due to damage of non-structural components is much more than that of structural damage. Falling of ceilings and other components may also cause death of occupants. Such failures due to the 2011 Great East Japan Earthquake were enormous.

Fig. 22 shows component acceleration spectra for the top floors of the four 29-, 21-, 41- and 54-story buildings. Damping ratio of the component is assumed to be 3%. The value attached to “original damping” is the first mode damping ratio. For 29-story Building (Fig. 22a) that is seismically resistant, the broken line is based on the recorded top floor acceleration of the original building having low damping ratios as mentioned earlier, and solid line shows a case where the building damping ratios of the first three modes are increased to 4%. In contrast, for 21-, 41- and 54-story buildings (Fig. 22b-d) that are supplementally-damped, the solid line is based on recorded top floor acceleration of the original building (Figs. 19 to 21), and the broken line shows when the first three modal damping ratios of the building are reduced to 1%. These examine a merit of increasing building modal damping ratios for protecting the acceleration-sensitive components.

According to Fig. 22, the past belief that short-period components are safer in a tall building is incorrect. They are as vulnerable as the long-period components due to multiple resonance peaks created by different modes of the building. The peaks are extremely high, even greater than $2,000 \text{ cm/s}^2$ ($\approx 2G$). Thus, the resonant acceleration of the components may be greater than $8G$ at a so-called major quake 4 times or

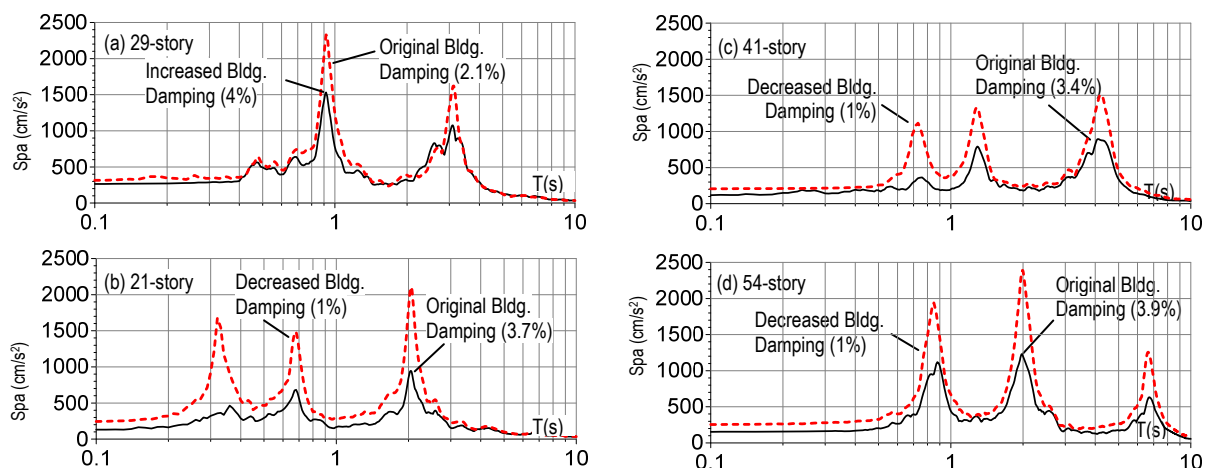


Figure 22 Component Response Spectra (Component Damping Ratio = 3%).

stronger. The problem may become more serious when damage and softening of components cause period shifting from one resonance peak to others. Note that three peaks for each building are shown in Fig. 22, since the first three modes were identified. But more peaks may emerge in an actual low damping case.

As a rule of thumb, facilities may overturn when floor acceleration exceeds 0.3G, and ceiling whose vibration period typically ranges from 0.3s to 1s may fall when its acceleration response exceeds 1G. These indicate the needs for an immediate attention to component responses at a major quake that will occur in Tokyo. Fig. 22 also clearly indicates that even moderately increasing the building damping ratio by 3% or so would reduce the component acceleration considerably.

5. SUMMARIES AND CONCLUSIONS

Based on two major studies, characteristics and performance of supplementally-damped buildings are discussed. Summaries and conclusions are as follows:

(1) Seismic responses of full-scale 5-story buildings with or without dampers were realistically simulated by the E-Defense shake-table, and numerous data for member-by-member responses and global responses were obtained for the range of minor to catastrophic levels of ground motions, all of which are important for examining design and analysis schemes. The results showed much better performance as compared with the building without dampers.

(2) The frame was tested repeatedly, by removing and inserting steel, viscous, oil, and viscoelastic dampers types in order. The dampers therefore were subjected to complicated three-dimensional motions, but they still performed as expected from individual damper tests that use highly idealized boundary conditions and produce key data for response-control design.

(3) The buildings with the different damper types can be designed to show similar displacements and accelerations at a specified earthquake level, but they behave differently at other levels due to different hysteretic characteristics of the dampers. The most prominent difference is seen from the steel damper case in which no or little energy is dissipated at smaller earthquakes.

(4) The performance of the building against different levels of seismic input can be quickly evaluated using the performance curves adopted by the current several Japanese specifications for designing against target performance. Force distributions among the frames and dampers at various seismic input levels can be also estimated by using the same steady-state theory as used for plotting performance curves.

(5) The equivalent damping ratio and vibration period are the key parameters for response-control design. In the two major studies presented, they were estimated commonly by a basic system identification method, assuming linear and proportional damping properties. Good agreement was found between the shake-table test records or actual earthquake observation records and the mode-superposition analyses using the identified properties.

(6) Although not described, the method summarized in (4) can be utilized as an alternative rule to estimate equivalent damping and period. It assumes ideal hysteresis of the dampers, and estimates loss of damper deformation and energy dissipation due

to deformations of connected members, and combines them with the modal strain energy method to obtain both equivalent damping and period. It gave similar results as in (5), and will be described elsewhere.

(7) Using the acceleration records of tall buildings in Tokyo during the 2011 Tohoku-Oki Earthquake, typical damping ratios of the conventional tall buildings and supplementally-damped tall buildings were reported. For the former as well as buildings with steel dampers described in (3), the ratio was between 0.01 and 0.02, and for the latter it was around 0.04.

(8) The observed responses of the buildings with velocity dependent dampers were compared with hypothetical analyses with damping ratio lowered to either 0.01 or 0.02. With the dampers, reduction of peak responses, significantly faster decay of vibration is observed, and these help reducing damage and fatigue of structural and non-structural components as well as fear of the occupants. In this regard, steel damper, although economical and effective for a major event, could be supplemented with velocity-dependent dampers for better performance-based design.

(9) By successfully analyzing contributions of multiple vibration modes, various shaking phenomena in the tall building that had not been experienced are clarified. Moreover, the most significant evidence of response-control effectiveness was presented, and the merit of damping technology for occupants and contents in the tall building is explained.

(10) Immediate attention must be given to mitigate acceleration-induced hazards in existing and new tall buildings against much stronger shaking likely to occur in the near future. The use of dampers appears to be desirable, since it can reduce not only peak accelerations but also number of large response cycles, and duration of significant shaking.

The present paper has discussed issues related to supplemental damping and response-control, focusing on global responses of the system. In order to assure such design, all members must be properly sized. Hence, designs for the components such as beams, columns, connections, and dampers are important and are currently studied by the writer and the colleagues.

ACKNOWLEDGEMENTS.

The writer acknowledges significant help provided by Dr. Matsuda, Assistant Professor of Tokyo Institute of Technology. The graduate students also assisted calculations, and they are Mr. Fujita, Mr. Sakaibara, Mr. Hasegawa, Mr. Yamamoto, and Mr. Chaya, Built Environment Department, TIT. Special thanks are given to Dr. Kani and Ms. Matsuda for their kind support.

REFERENCES.

- [1] Kasai, K., Fu, Y., and Watanabe, A. (1998), "Passive Control Systems for Seismic Damage Mitigation," *Journal of Structural Engineering*, American Society of Civil Engineers, 124(5), 501-512.
- [2] Fu, Y. and Kasai, K., (1998), "Comparative Study of Frames Using Viscoelastic

and Viscous Dampers”, J. Struct. Eng., American Society of Civil Engineers, 122 [10], pp. 513-522

[3] JSSI Manual (2003, 2005, 2007), Design and Construction Manual for Passively Controlled Buildings, Japan Society of Seismic Isolation (JSSI), Tokyo, Japan.

[4] Kasai, K., and Ito, H. (2005): Passive Control Design Method Based on Tuning of Stiffness, Yield Strength, and Ductility of Elasto-plastic Damper, J. Struct. Constr. Eng., AIJ, Vol. 70, No. 595, pp.45-55, (in Japanese).

[5] Kasai, K. and Iwasaki, K. (2006a): “Reduced Expression for Various Passive Control Systems and Conversion to Shear Spring Model”, Journal of Structural and Construction Engineering, No.605, pp.37-46 (In Japanese)

[6] Kasai, K., Minato, N., and Kawanabe, Y. (2006b): Passive Control Design Method Based on Tuning of Equivalent Stiffness of Visco-elastic Damper, J. Struct. Constr. Eng., AIJ, Vol. 71, No. 610, pp.75-83, (in Japanese).

[7] Kasai, K., Ogura, T., and Suzuki, A. (2007): Passive Control Design Method Based on Tuning of Equivalent Stiffness of Nonlinear Viscous Damper, J. Struct. Constr. Eng., AIJ, Vol. 72, No. 618, pp.97-104, (in Japanese).

[8] Kasai, K., Ito, H., and Ogura, T. (2008a): Passive Control Design Method Based on Tuning of Equivalent Stiffness of Bilinear Oil Damper, J. Struct. Constr. Eng., AIJ, Vol. 73, No. 630, pp.1281-1288, (in Japanese).

[9] Kasai, K., Ooki, Y., Ishii, M., Ozaki, H., Ito H., Motoyui S., Hikino, T., and Sato, E. (2008b): Value-Added 5-Story Steel Frame and Its Components; Part 1 – Full-Scale Damper Tests and Analysis, S17-01-013, The 14th World Conference on Earthquake Engineering, Beijing, Oct. 12-17

[10] Ooki, Y., Kasai, K., Azuma, Y., Motoyui, S., and Kaneko, K. (2008): Value-Added 5-Story Steel Frame and Its Components: Part 2 – Full-Scale Tests of Beam-Column-Gusset Plate Assemblies, S17-01-015, The 14th World Conference on Earthquake Engineering, Beijing, Oct. 12-17

[11] Kasai, K., Motoyui, S., Ozaki, H., Ishii, M., Ito, H., Kajiwara, K., and Hikino, T. (2009a): Full-Scale Tests of Passively-Controlled 5-Story Steel Building Using E-Defense Shake Table, Part 1: Test concept, method, and building specimen, Proc. of STESSA 2009, Keynote Paper, pp. 11-17, Philadelphia.

[12] Kasai, K., Ooki, Y., Ito, H., and Motoyui, S., Hikino, T. and Sato, E. (2009b): Full-Scale Tests of Passively-Controlled 5-Story Steel Building Using E-Defense Shake Table, Part 2: Preliminary Analysis Results, Proc. of STESSA 2009, pp. 87-92, Philadelphia.

[13] Ooki, Y., Kasai, K., Motoyui, S., Kaneko, K., Kajiwara, K., and Hikino, T. (2009): Full-Scale Tests of Passively-Controlled 5-Story Steel Building Using E-Defense Shake Table, Part 3: Full-Scale Tests for Dampers and Beam-Column Subassemblies, Proc. of STESSA 2009, pp. 93-99, Philadelphia.

[14] Yamada, S, Suita, K, Tada, M, Kasai, K, Matsuoka, Y, and Shimada, Y. (2009): Full Scale Shaking Table Collapse Experiment on 4-Story Steel Moment Frame: Part 1 Outline of the Experiment, Proc. of STESSA 2009, pp. 11-17, Philadelphia.

[15] Suita, K, Yamada, S, Kasai, K, Shimada, Y, Tada, M, and Matsuoka, Y. (2009): Full Scale Shaking Table Collapse Experiment on 4-Story Steel Moment Frame: Part 2 Detail of Collapse Behavior, Proc. of STESSA 2009, pp. 131-136, Philadelphia, 2009

[16] Kasai, K., Hikino, T., Ito, H., Ooki, Y., Motoyui, S., Kato, F., and Baba, Y. (2011a): Overall Test Outline and Response of Building without Dampers, Part 1: 3D

Shake Table Tests on Full Scale 5-Story Steel Building with Dampers, J. Struct. Constr. Eng., AIJ, Vol. 76, No. 663, pp.997-1006. (in Japanese).

[17] Kasai, K., Murata, S., Kato, F., Hikino, T., and Ooki, Y. (2011b): Evaluation Rule for Vibration Period, Damping, and Mode Vector of Buildings Tested by A Shake Table with Inevitable Rocking Motions, J. Struct. Constr. Eng., AIJ, Vol. 76, No. 670, pp.2031-2040. (in Japanese).

[18] Kasai, K. (2011c): 4.2.3 Acceleration Records of Buildings, 4.4.5. Behavior of Response Controlled Buildings, Preliminary Reconnaissance Report of the 2011 Tohoku-Chiho Taiheiyo-Oki Earthquake, Architectural Institute of Japan, pp.280-284, pp.345-347 (in Japanese).

[19] Kasai, K. (2011d): Chapter 4. Performance of Response-Controlled Buildings, The Kenchiku Gijutsu, No.741, pp.118-123. (in Japanese).

[20] Koyama, S., and Kashima, T. (2011): Prompt Report on Strong Motions Recorded during the 2011 Tohoku Pacific Ocean Earthquake, Report 5, Building Research Institute (BRI).

[21] Maseki, R., Nii, A., Nagashima, I., Aono, H., Kimura, Y., and Hosozawa, O. (2011): Performance of Seismic Retrofitting of Suoer High-Rise Building Based on Earthquake Observation Records, International Symposium on Disaster Simulation and Structural Safety in the Next Generation (DS'11), Japan

[22] Hisada, Y., Kubo, T., and Yamashita, T. (2011): Shaking and Damage of the Shinjuku Campus Building and Shinjuku Campus Report from Kougakuin University, Internet Access (in Japanese):

http://kouzou.cc.kogakuin.ac.jp/Open/20110420Event/20Apr11_Kogakuin01.pdf

[23] Hisada, Y., Yamashita, T., Murakami, M., Kubo, T., Shindo, J., Aizawa K., and Arata T. (2012): Sesimic Response and Damage of High-Rise Buildings in Tokyo, Japan During the Great East Japan Earthquake, Proceedings, International Symposium on Engineering Lessons Learned from the Giant Earthquake, Tokyo, Japan, March 3 -4.

[24] Kasai, K., Baba, Y., Nishizawa, K., Hikino, T., Ito, H., Ooki, Y., and Motoyui, S. (2012a): Test Results for Building with Steel Dampers, Part 2: 3D Shake Table Tests on Full Scale 5-Story Steel Building with Dampers, J. Struct. Constr. Eng., AIJ, Vol. 77, No. 673, pp.499-508. (in Japanese).

[25] Kasai, K., Baba, Y., Ito, H., Tokoro, K., Hikino, T., Ooki, Y., and Murai, R. (2012b): 3-D Shake Table Tests on Full-Scale 5-Story Steel Building with Viscoelastic Dampers, J. Struct. Constr. Eng., AIJ, Vol. 77, No. 676, pp.985-994, (in Japanese).

[26] Kasai, K., Pu, W., and Wada, A. (2012c): Responses of Tall Buildings in Tokyo during the 2011 Great East Japan Earthquake, Proc. of STESSA 2012 (Behaviour of steel structures in seismic areas), Keynote Paper, pp.25-35, Santiago, Chile, 9-11 January.

[27] Kasai, K. (2012d): Seismic Performance of Buildings with Dampers: Evaluation From Full-Scale Specimen Test and Actual Building Monitoring, International Workshop on Advances in Seismic Experiments and Computations (ASEC2012), Keynote Paper, Nagoya, Japan, 12-13 March, 2012

[28] Kasai, K., Mita, A., Kitamura, H., Matsuda, K., Morgan, T., and Taylor, A., (2013): Performance of Seismic Protection Technologies During the 2011 Tohoku-Oki Earthquake, Earthquake Spectra, Special Issue on the 2011 Tohoku-Oki Earthquake and Tsunami, pp.265-294